OPEN

Formation of Graphene Grain Boundaries on Cu(100) Surface and a Route Towards Their Elimination in Chemical Vapor Deposition Growth

Qinghong Yuan[1,2], Guangyao Song[1], Deyan Sun[1] & Feng Ding[3]

[1]Department of Physics, East China Normal University, Shanghai, China, [2]Key laboratory of Computational Physical Sciences (Fudan University), Ministry of Education, Shanghai, China, [3]Institute of Textiles and Clothing, Hong Kong Polytechnic University, Kowloon, Hong Kong, Peoples Republic of China.

Grain boundaries (GBs) in graphene prepared by chemical vapor deposition (CVD) greatly degrade the electrical and mechanical properties of graphene and thus hinder the applications of graphene in electronic devices. The seamless stitching of graphene flakes can avoid GBs, wherein the identical orientation of graphene domain is required. In this letter, the graphene orientation on one of the most used catalyst surface — Cu(100) surface, is explored by density functional theory (DFT) calculations. Our calculation demonstrates that a zigzag edged hexagonal graphene domain on a Cu(100) surface has two equivalent energetically preferred orientations, which are 30 degree away from each other. Therefore, the fusion of graphene domains on Cu(100) surface during CVD growth will inevitably lead to densely distributed GBs in the synthesized graphene. Aiming to solve this problem, a simple route, that applies external strain to break the symmetry of the Cu(100) surface, was proposed and proved efficient.

G raphene is the most promising material for the next-generation electronics. Its application requires the production of large-area graphene with low defect concentration and high uniformity. The chemical vapour deposition (CVD) synthesis of graphene on Cu substrate[1–5] is regarded as the most practical method to achieve the above mentioned requirement. Although great progresses have been made, such as the synthesis of 30 inches single layer graphene sheet on Cu surface have been achieved[2], the mobility of the CVD graphene samples is still far from expected. It is broadly believed that the grain boundaries (GBs) formed during CVD growth are responsible for the great deduction of graphene's electronic performances[6–14]. During the graphene CVD growth, the GBs are mainly formed by the coalescence of graphene domains[14–17]. In experiment, the main strategy for obtaining graphene with less GBs is to reduce the nucleation density, which can be realized by using low pressure CH$_4$ as feedstock[18–21] or introducing oxygen into growth process[22]. But such a strategy suffers from a very slow growth rate which is a great drawback. For example, the growth of a single crystalline graphene domain from the length of nm to cm may cost a few days[20,23]. Another possible approach to obtain graphene with less GBs is to stitch several graphene domains seamlessly, which requires all graphene domains possess the identical orientation on the catalyst surface. Cu(100) surface is the most used catalyst surface during graphene CVD growth. Graphene domains formed on the Cu(100) surface are normally not well aligned and GBs are observed to distribute densely and broadly[24–28]. Therefore, in order to obtain GB-free graphene on Cu(100) surface, it is crucial to achieve a comprehensive understanding about the formation mechanism of GBs and the key factors that control the graphene orientation.

Under thermodynamic equilibrium conditions, the probability of forming a small graphene island on a catalyst surface can be estimated by

$$P \sim \exp\left(-\frac{E_f}{k_b T}\right) \qquad (1)$$

where E_f is the formation energy of the graphene domain, k_b is the Boltzmann constant and T is the temperature. Considering the orientation of a very large graphene domain is hard to be changed, the orientation of a graphene domain should be determined by the low energy directions at the infant stage[29]. To find out the most favorable
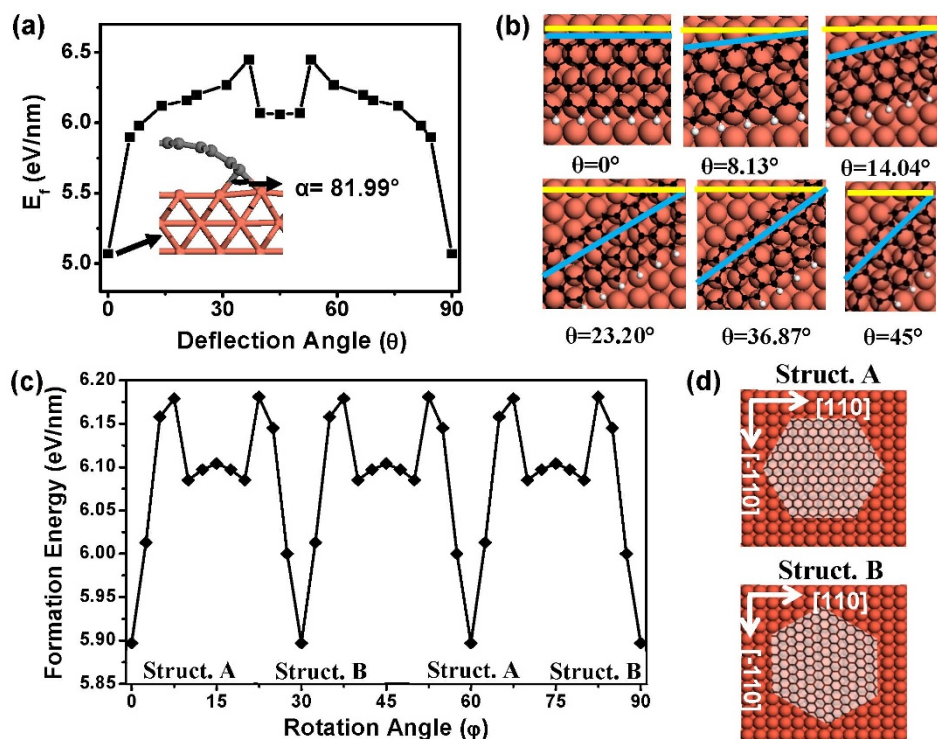
Figure 1 | (a) Formation energies and (b) optimized geometries of a graphene ZZ edge on the Cu(100) surface with binding orientation of θ = 0°, 8.13°, 14.04°, 23.20°, 36.87° and 45°. The values for θ > 45° are determined by the symmetry of the system. (c) Formation energy vs. rotation angle of a hexagonal graphene domain on Cu(100) surface. (d) geometries of **Struct. A** and **Struct B** appeared in (c).

graphene orientation on Cu(100) surface, the graphene orientation with the lowest E_f value must be determined. However, directly comparing the formation energies of graphene domains with different orientations is difficult because of the requirement of huge computational models. Previous experimental observations and theoretical predictions have confirmed that graphene flakes under equilibrium conditions preferred the regular zigzag (ZZ) edges because of its low growth rate and low formation energy[30–35]. Another theoretical study has shown that the graphene-catalyst interaction is dominated by the strong edge-catalyst interaction instead of the weak Van der Waals (VDW) interaction between graphene wall and the catalyst surface[29]. Therefore, we propose to build up a growing graphene island as a hexagonal graphene domain with six zigzag edges and calculate the graphene edge-catalyst interaction as the summation of interactions between the six graphene ZZ edges and the Cu(100) catalyst surface.

In this letter, the most favorable orientation of a ZZ edged hexagonal graphene on Cu(100) surface is systematically explored. Our theoretical calculations demonstrate that a graphene ZZ edge has two identical stable orientations, [110] or [−110] direction of the Cu(100) surface. Hence, the coalescence of graphene domains on the Cu(100) surface will inevitablly leads to high concentrated GBs. We further showed that the external axial compressive strain along one of the [110] and [−110] direction can reduce the symmetry of the system to C_2 and notably increase the energy difference of the two directions. And thus a simple route of suppressing one of the two equivalent orientations during graphene CVD growth on Cu(100) surface is proposed and expected to be applied during graphene CVD growth.

Results

To locate the optimum orientation of graphene domain on Cu(100) surface, we firstly explored the binding between a graphene ZZ edge and the surface as a function of the edge's orientation. Neglecting the small lattice mismatching between graphene and Cu(100) surface (~4%), a graphene ZZ edge can be perfectly placed along the [110]

direction of Cu(100) surface, as shown by θ = 0° in Figure 1b. Here, the binding orientation angel, θ, is defined as the deflection angle between the graphene ZZ edge and the [110] direction of the Cu(100) surface. Considering the C_4 symmetry of Cu(100) surface, the deflection angle, θ, on the Cu(100) surface has a periodicity of 90°, in which θ to the [110] direction should be equivalent to 90° − θ to the [−110] direction because of the equivalence of the [110] and [−110] direction. Thus the investigated deflection angle only varies from 0° to 45°, and there are 10 different θ values are studied. For each θ, the formation energy of the ZZ edge, E_{ZZ}, on the Cu(100) surface was calculated as

$$E_{ZZ} = \left(E_{GNR/Cu100} - E_{Cu100} - E_{GNR} \right)/L \qquad (2)$$

where $E_{GNR/Cu100}$, E_{Cu100} and E_{GNR} are the energies of graphene nanoribbon (GNR) adsorbed on the Cu(100) surface, the Cu(100) substrate and the isolated GNR, respectively, and L is the length of GNR's edge.

The calculated formation energies and several optimized geometries of graphene ZZ edge on Cu(100) surface are shown in Figure 1a and 1b, respectively. It can be seen that the formation energy of the ZZ edge increases dramatically when θ goes up from zero. For example, $E_{ZZ}(θ)$ increases from 5.17 eV to 5.87 eV as θ increases from 0° to 5.71°. While the energy change becomes very slow when θ is larger than 5.71°. E.g. the formation energy changes only 0.58 eV when θ varies from 5.71° to 36.87°. This demonstrated that ZZ edges with the orientation of θ = 0° + i * 90° (i is an integer) are the most favorable orientations on the Cu(100) surface. This is due to the favorable binding site of the edge C atoms. For θ = 0° + i * 90°, the commensurate system has a very small unit cell size of 0.246 nm, which allows each edge C atom to be located at a bridge site of the [100] surface (Figure 1b). Binding at the bridge site leads to the formation of two Cu-C bonds perpendicular to the graphene edge (inset of Figure 1a). This is energetically favorable because the edge C atom is sp³ hybridized and the two dangling bonds can be effectively saturated. However, when a ZZ edge rotates away from the [110]
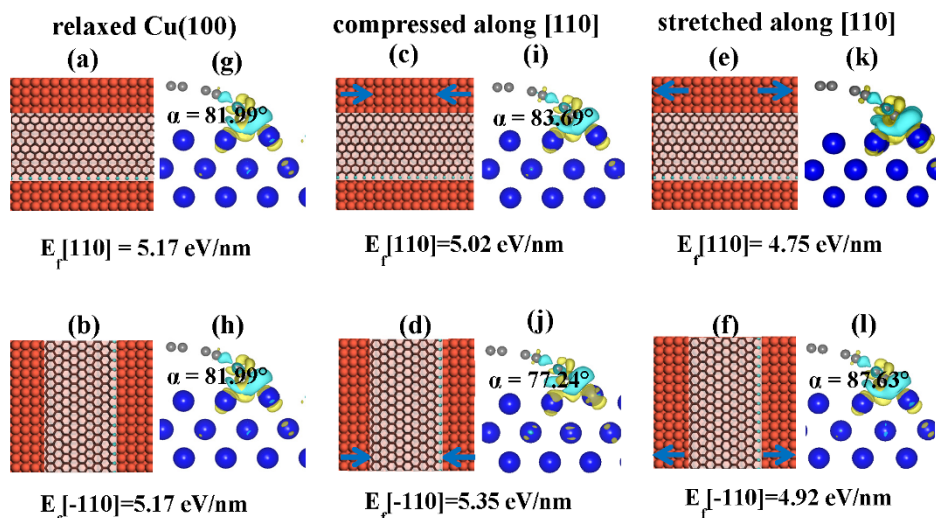
Figure 2 | Formation energy and charge density difference (CDD) of graphene ZZ edge binding along (a,g) [110] direction and (b,h) [−110] direction of free Cu(100); (c,i) [110] direction and (d,j) [−110] direction of 4% partially compressed Cu(100); (e,k) [110] direction and (f,l) [−110] direction of 5% partially stretched Cu(100).

direction, some edge C atoms have to be deviated from the bridge sites, e.g., for $\theta = 5.71°$ (shown in Figure S1), and thus the energy will increase. Different from that of the bridge site, an edge C atom binds on a top site has high formation energy because only one of the dangling bonds is saturated (shown in Figure S2). It is worth mentioning that, a lattice approximation between graphene and the Cu substrate was used for $\theta = 0°$ in order to reduce the computational model to acceptable size. Perfect lattice matching leads to the deviating of some edge C atoms from the Cu-Cu bridge site but the edge C atoms never bind on the top site of Cu atom. Thus it can be concluded that $\theta = 0°$ remaines as the most favorable orientation even if the perfect lattice matching is taken into account. (detailed discussion and analysis can be found in SI-3 of SI).

Based on the obtained orientation dependent formation energy of a graphene ZZ edge on the Cu(100) surface (Figure 1a), the formation energy of a graphene domain with certain orientation on the same catalyst surface can be easily obtained. For a most frequently observed hexagonal graphene domain on the Cu(100) surface[1,20,23,31,36,37], the graphene-Cu(100) [G/Cu(100)] system has a symmetry of C_2, as shown by **Struct. A** in Figure 1d. In this C_2 symmetric structure, two graphene ZZ edges perfectly aligned with the [110] direction of Cu(100) surface, and the other four graphene edges deviate by 60° and −60° from the [110] direction, respectively. When the graphene domain in **Struct. A** is rotated by φ degree in relative to the Cu(100) substrate, the orientations of the six ZZ edges of graphene are φ, $60° + \varphi$, and $−60° + \varphi$, respectively. Therefore, the formation energy of the hexagonal graphene domain, $E_{hex}(\varphi)$, can be written as

$$E_{hex}(\varphi) = [2E_{ZZ}(\varphi) + 2E_{ZZ}(−60° + \varphi) + 2E_{ZZ}(60° + \varphi)]/6 \quad (0° \leq \varphi \leq 60°) (3)$$

where $E_{ZZ}(\varphi)$ is a function of φ with a periodicity of $\pi/2$ as shown in Figure 1a. Based on the calculated $E_{ZZ}(\varphi)$ and Eq. (3), we can plot the formation energy of the hexagonal graphene domain, E_{hex}, as a function of φ by using linear interpolation (Figure 1c). In contrast to $E_{ZZ}(\varphi)$ which has a periodicity of $\pi/2$, the $E_{hex}(\varphi)$ has a periodicity of $\pi/6$. There are four local minimums of $E_{hex}(\varphi)$ in the range of $0° \leq \varphi \leq 90°$, which appear at $\varphi = 0°$, 30°, 60° and 90° respectively. The structure with $\varphi = 0°$ or 60° corresponds to **Struct. A** and the structure with $\varphi = 30°$ or 90° corresponds to **Struct. B** as shown in Figure 1c. On the Cu(100) surface, both **Struct. A** and **B** have two graphene ZZ edges binding along the [110]/[−110] direction and four graphene ZZ edges deviated by 60° from the [110] or [−110]

direction (Figure 1d). Given that the [110] and [−110] directions are equivalent on Cu(100) surface, the **Struct. A** and **B** are also equivalent. Therefore, a graphene domain on Cu(100) surface has two favorable orientations, which are rotated by 30° from each other.

For graphene nucleated on the Cu(100) surface, the populations of domains with two equivalent orientations must have very similar probability and thus the seamless fusion of graphene domains is impossible. As a consequence, large-area graphene sheet grown on Cu(100) surface normally have many GBs, which is consistent with many experimental observations[5,24–27,38].

Aligning the graphene domains along a specific orientation on Cu(100) surface is essential to achieve the seamless fusion of graphene domains and is the key to improve the quality of the synthesized graphene. It's important to note that the C_4 symmetry of Cu(100) surface is responsible for the two equivalent orientations. If the C_4 symmetry of the Cu(100) surface was broken or the [110] and [−110] directions are no longer equivalent, the two different graphene structures would be non-equivalent as well. In order to break the C_4 symmetry of the Cu(100) surface, here we propose to apply an external strain along one of the [110] and [−110] directions. With such an external strain, the lattice constant along one direction would be different from that along the other one. Thus the symmetry of the Cu(100) surface will be reduced to C_2 and the degenerated **Struct. A** and **B** are no longer equivalent.

To determine whether the stability of the graphene ZZ edge is sensitive to the external strain, we firstly compared the formation energies of the graphene ZZ edge on the Cu(100) surface compressed/stretched along [110] direction (Figure 2). According to the Poisson's ratio of Cu substrate, the [−110] direction of the Cu(100) substrate is slightly stretched/compressed as the [110] direction of the Cu(100) substrate is compressed/stretched. (the computational details can be found in SI-5 of SI) On a compressed Cu(100) surface with −4% strain, the formation energy of graphene ZZ edge binding along the [110] direction is decreased to 5.02 eV/nm, whereas it is increased to 5.35 ev/nm for ZZ edge binding along the [−110] direction. (Figure 2c–d) The formation energy difference of ZZ edge along [110] and [−110] directions can be attributed to the different bond angle of the edge C atom. As we know, a sp³ hybridized C atom has four covalent bonds and the preferred bond angle is ~109°. The larger the α deviates from 109°, the higher formation energy the edge C atom has. For the edge C atom binding along the [110]/[−110] direction of relaxed Cu(100) surface, the bond angle α

is 81.99° (Figure 1g–h). The α increases to 83.69° when the [110] direction is compressed by 4%, as shown in Figure 2i. Accordingly, the binding of the ZZ edge becomes stronger. On the contrary, the bond angle of ZZ edge along the [−110] direction decreases to 77.24° (Figure 3j) because of the ristricted distance of the two Cu atoms along the [110] direction. This leads to a higher formation energy of ZZ edge along the [−110] direction. The binding strength can also be seen from the charge density difference (CDD) analysis (Figure 2g–l), the stronger binding corresponds to a larger charge transfer from the Cu substrate to the edge of GNR. Compared with the equal charge transfer along [110]/[−110] direction of relaxed Cu(100) surface, charge transfer on the compressed Cu(100) surface is increased along the [110] direction but decreased along the [−110] direction (Figure 2g–j). This leads to a lower formation energy of ZZ edge along the [110] direction but a higher formation energy along the [−110] direction. However, the situation is slightly different for ZZ edge on a stretched Cu(100) surface with 5% strain. The calculated formation energies of a ZZ edge binding along both the [110] and [−110] directions are decreased (4.75 and 4.92 eV/nm for [110] and [−110] direction, respectively) since charge transfer on both directions is increased. The energy difference of the ZZ edges binding along the [110] and [−110] direction of the compressed Cu(100) surface is as large as 0.33 eV/nm, while the energy difference is only 0.17 eV/nm on the stretched Cu(100) surface.

From the above calculations, we can conclude that the relative stability of graphene edge is more sensitive to the compressive strain and thus we propose to use the compressive strain to suppress one of the **Struct. A** and **B** on the Cu(100) surface.

To confirm the hypothesis, we further calculated the formation energies of graphene ZZ edge along different directions on a compressed Cu(100) surface. Considering the C_2 symmetry of the com-

pressed Cu(100) surface, we investigated the deflection angle θ which is changed from 0° to 180°. On the compressed Cu(100) surface, the calculated formation energies of graphene ZZ edge along the [110] and [−110] directions (0° and 90° respectively, as shown in Figure 3a) are not degenerate any more, which is consistent with our prediction.

Based on the calculated $E_{ZZ}(\theta)$ on a compressed Cu(100) surface (Figure 3a) and Eq. (3), the E_{hex} on a compressed Cu(100) surface as a function of φ can be obtained (Figure 3b). In contrast to the situation on the relaxed Cu(100) surface, the periodicity of $E_{hex}(\varphi)$ on a compressed Cu(100) surface become $\pi/3$ due to the change of the symmetry. There are four global minima and three local minima of $E_{hex}(\varphi)$ can be identified in the range of $0° \leq \varphi \leq 180°$ due to the energy separation of **Struct. A** and **B**. The four global minima appear at $\varphi = 0°, 60°, 120°$ and $180°$ are corresponding to **Struct. A** as shown in Figure 1d. The three local minima appear at $\varphi = 30°, 90°, 150°$ correspond to **Struct. B**. For a hexagonal graphene domain with the edge length of 2 nm, the formation energy of **Struct. A** is ~1.2 eV/nm lower than that of **Struct. B**. This should leads to a large population of **Struct. A** domains on the compressed Cu(100) surface. Assuming such a graphene domain can be freely rotated at the experimental temperature of 1200 K, the population difference of the two structures can be roughly estimated by exp(1.2 eV/kT) ~ 10⁵, which indicating a great suppression of **Struct. B** in the synthesized graphene domains. To further verify the conclusion, we calculate the formation energies of two differently oriented small hexagonal graphene flakes (C_{54}) on a 4% compressed Cu(100) surface. Our calculation shows that the hexagonal C_{54} with two ZZ edges bound along the compressed [110] direction is 1.29 eV lower than C_{54} with two ZZ edges bound along the [−110] direction (the optimized structures and formation energies can be found in Figure S2 of SI).

Based on the above discussion, we can see that a graphene domains on the Cu(100) surface have two equivalent orientations rotated by 30°. Thus, fusion of graphene domains grown on the Cu(100) surface must lead to numerous GBs (Figure 4a). In order to avoid the formation of GBs during graphene domain fusion, uniformly aligning the graphene domains is required. By imposing a compressive strain along one of the [110] and [−110] directions, one of the two equivalent graphene orientations could be greatly suppressed and therefore the formation of GBs during the fusion of the graphene domains can be avoided. Through such a process, the quick synthesis of large-area and high-quality graphene is possible (Figure 4b).

In conclusion, our theoretical calculations demonstrate that the graphene ZZ edge has the lowest formation energy when it binds
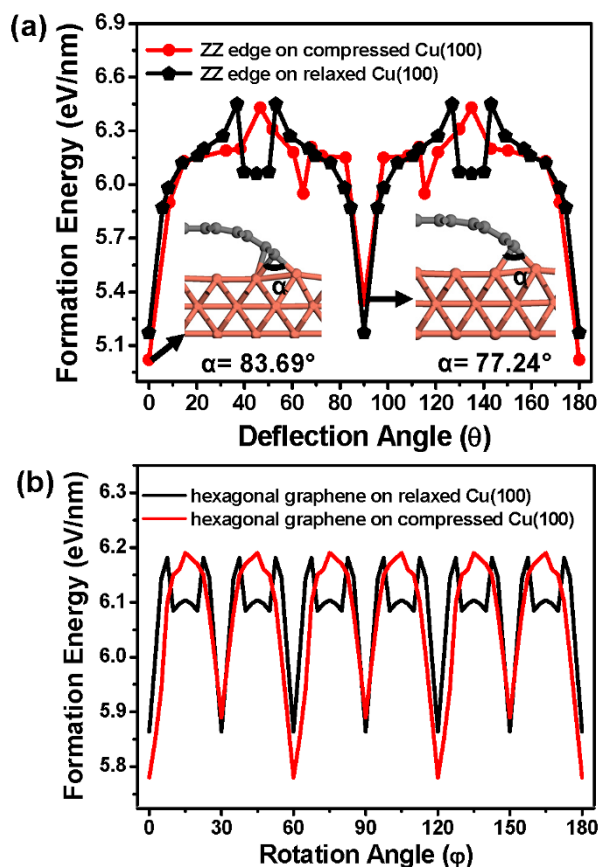

Figure 3 | Formation energies of (a) graphene ZZ edge and (b) hexagonal graphene domain on relaxed and 4% compressed Cu(100) surfaces.
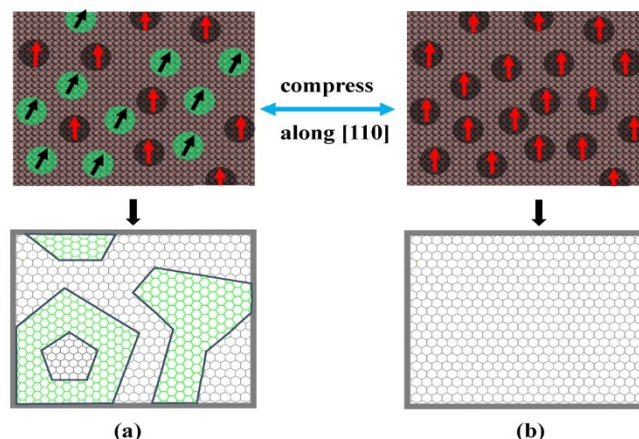

Figure 4 | (a) Incommensurate graphene growth on relaxed Cu(100) surface because of the two equivalent graphene orientations (black circle represents 0° oriented graphene domain, green circle represents 30° oriented graphene domain); (b) Commensurate growth of graphene on compressed Cu(100) surface.

along the [110]/[−110] direction of Cu(100) surface. The two optimum binding orientations of a ZZ edge leads to two equivalent stable orientations of a hexagonal graphene domains on the Cu(100) surface. By imposing compression on Cu(100) surface along the [110] or [−110] direction, the two degenerated orientations are well separated and a strategy of achieving seamless graphene on the Cu(100) surface is emerged.

Methods

To describe the binding of graphene ZZ edge on free and compressed/stretched Cu(100) surfaces, models with periodic boundary conditions (PBC) are carefully designed. The graphene ZZ edge is represented by a ZZ graphene nanoribbon (GNR) with one edge saturated by H atoms. And the width of the GNR is 8.13 Å which including 3 hexagonal rings along the width direction. GNR with larger width is also adopted in our calculations and the calculated formation energy is almost the same as that of GNR with width of 8.13 Å. Thus the GNR with width of 8.13 Å was used in most of our calculations. All calculations performed are based on the density functional theory (DFT) implemented in the Vienna Ab-initio Simulation Package (VASP)[39,40]. Electronic exchange and correlation were included through the generalized gradient approximation (GGA) in the Perdew–Burke–Ernzerhof (PBE) form[41]. The projector-augmented wave (PAW) method was used to describe the electronic interaction. Spin unpolarized calculations were adopted with a plane-wave kinetic-energy cutoff of 400 eV. For large super-cells with size larger than $15 \times 15 \times 15$ Å^3, the Brillouin zone was sampled only at the Γ point. While for small super-cells, multiple K points were used. All structures were optimized until the maximum force component on each atom was less than 0.02 eV/Å. Similar calculation setups have been extensively implemented in our previous studies and were proved reliable[42,43].

1. Li, X. S. et al. Large-Area Synthesis of High-Quality and Uniform Graphene Films on Copper Foils. Science 324, 1312–1314 (2009).
2. Bae, S. et al. Roll-to-roll production of 30-inch graphene films for transparent electrodes. Nat. Nanotechnol. 5, 574–578 (2010).
3. Gao, L., Guest, J. R. & Guisinger, N. P. Epitaxial Graphene on Cu(111). Nano Lett. 10, 3512–3516 (2010).
4. Mattevi, C., Kim, H. & Chhowalla, M. A review of chemical vapour deposition of graphene on copper. J. Mater. Chem. 21, 3324–3334 (2011).
5. Wood, J. D., Schmucker, S. W., Lyons, A. S., Pop, E. & Lyding, J. W. Effects of Polycrystalline Cu Substrate on Graphene Growth by Chemical Vapor Deposition. Nano Lett. 11, 4547–4554 (2011).
6. Falvo, M. R. et al. Bending and buckling of carbon nanotubes under large strain. Nature 389, 582–584 (1997).
7. Yu, Q. K. et al. Control and characterization of individual grains and grain boundaries in graphene grown by chemical vapour deposition. Nat. Mater. 10, 443–449 (2011).
8. Yazyev, O. V. & Louie, S. G. Electronic transport in polycrystalline graphene. Nat. Mater. 9, 806–809 (2010).
9. Lahiri, J., Lin, Y., Bozkurt, P., Oleynik, II & Batzill, M. An extended defect in graphene as a metallic wire. Nat. Nanotechnol. 5, 326–329 (2010).
10. Qi, Z. N. & Park, H. S. Intrinsic energy dissipation in CVD-grown graphene nanoresonators. Nanoscale 4, 3460–3465 (2012).
11. Huang, P. Y. et al. Grains and grain boundaries in single-layer graphene atomic patchwork quilts. Nature 469, 389–392 (2011).
12. Tsen, A. W. et al. Tailoring Electrical Transport Across Grain Boundaries in Polycrystalline Graphene. Science 336, 1143–1146 (2012).
13. Kim, D. W., Kim, Y. H., Jeong, H. S. & Jung, H. T. Direct visualization of large-area graphene domains and boundaries by optical birefringency. Nat. Nanotechnol. 7, 29–34 (2012).
14. Yakobson, B. I. & Ding, F. Observational Geology of Graphene, at the Nanoscale. Acs Nano 5, 1569–1574 (2011).
15. Kim, K. S. et al. Large-scale pattern growth of graphene films for stretchable transparent electrodes. Nature 457, 706–710 (2009).
16. Li, X. S. et al. Graphene Films with Large Domain Size by a Two-Step Chemical Vapor Deposition Process. Nano Lett. 10, 4328–4334 (2010).
17. Rasool, H. I. et al. Atomic-Scale Characterization of Graphene Grown on Copper (100) Single Crystals. J. Am. Chem. Soc. 133, 12536–12543 (2011).
18. Gao, J. F., Yuan, Q. H., Hu, H., Zhao, J. J. & Ding, F. Formation of Carbon Clusters in the Initial Stage of Chemical Vapor Deposition Graphene Growth on Ni(111) Surface. J. Phys. Chem. C 115, 17695–17703 (2011).
19. Kim, H. et al. Activation Energy Paths for Graphene Nucleation and Growth on Cu. Acs Nano 6, 3614–3623 (2012).
20. Wu, B. et al. Equiangular Hexagon-Shape-Controlled Synthesis of Graphene on Copper Surface. Adv. Mater. 23, 3522–3525 (2011).
21. Li, X. et al. Large-Area Graphene Single Crystals Grown by Low-Pressure Chemical Vapor Deposition of Methane on Copper. J. Am. Chem. Soc. 133, 2816–2819 (2011).
22. Hao, Y. et al. The Role of Surface Oxygen in the Growth of Large Single-Crystal Graphene on Copper. Science 342, 720–723 (2013).
23. Robertson, A. W. & Warner, J. H. Hexagonal Single Crystal Domains of Few-Layer Graphene on Copper Foils. Nano Lett. 11, 1182–1189 (2011).
24. Ogawa, Y. et al. Domain Structure and Boundary in Single-Layer Graphene Grown on Cu(111) and Cu(100) Films. J. Phys. Chem. Lett. 3, 219–226 (2012).
25. Ago, H., Ogawa, Y., Tsuji, M., Mizuno, S. & Hibino, H. Catalytic Growth of Graphene: Toward Large-Area Single-Crystalline Graphene. J. Phys. Chem. Lett. 3, 2228–2236 (2012).
26. Tao, L. et al. Synthesis of High Quality Monolayer Graphene at Reduced Temperature on Hydrogen-Enriched Evaporated Copper (111) Films. Acs Nano 6, 2319–2325 (2012).
27. Zhao, L. et al. Influence of copper crystal surface on the CVD growth of large area monolayer graphene. Solid State Commun. 151, 509–513 (2011).
28. Murdock, A. T. et al. Controlling the Orientation, Edge Geometry, and Thickness of Chemical Vapor Deposition Graphene. Acs Nano 7, 1351–1359 (2013).
29. Zhang, X., Xu, Z., Hui, L., Xin, J. & Ding, F. How the Orientation of Graphene Is Determined during Chemical Vapor Deposition Growth. J. Phys. Chem. Lett. 3, 2822–2827 (2012).
30. Gao, J. F., Zhao, J. J. & Ding, F. Transition Metal Surface Passivation Induced Graphene Edge Reconstruction. Journal of the American Chemical Society 134, 6204–6209 (2012).
31. Artyukhov, V. I., Liu, Y. Y. & Yakobson, B. I. Equilibrium at the edge and atomistic mechanisms of graphene growth. Proc. Natl. Acad. Sci. U S A 109, 15136–15140 (2012).
32. Shu, H. B., Chen, X. S., Tao, X. M. & Ding, F. Edges Structural Stability and Growth Kinetics of Graphene Chemical Vapor Deposition (CVD). Acs Nano 6, 3243–3250 (2012).
33. Fan, L. L. et al. Controllable growth of shaped graphene domains by atmospheric pressure chemical vapour deposition. Nanoscale 3, 4946–4950 (2011).
34. Luo, Z. T., Kim, S., Kawamoto, N., Rappe, A. M. & Johnson, A. T. C. Growth Mechanism of Hexagonal-Shape Graphene Flakes with Zigzag Edges. Acs Nano 5, 9154–9160 (2011).
35. Wu, P. et al. Lattice Mismatch Induced Nonlinear Growth of Graphene. J. Am. Chem. Soc. 134, 6045–6051 (2012).
36. Geng, D. C. et al. Uniform hexagonal graphene flakes and films grown on liquid copper surface. Proc. Natl. Acad. Sci. U S A 109, 7992–7996 (2012).
37. Yan, Z. et al. Toward the Synthesis of Wafer-Scale Single-Crystal Graphene on Copper Foils. Acs Nano 6, 9110–9117 (2012).
38. An, J. H. et al. Domain (Grain) Boundaries and Evidence of "Twinlike" Structures in Chemically Vapor Deposited Grown Graphene. Acs Nano 5, 2433–2439 (2011).
39. Kresse, G. & Furthmuller, J. Efficiency of ab-initio total energy calculations for metals and semiconductors using a plane-wave basis set. Comput. Mater. Sci. 6, 15–50 (1996).
40. Kresse, G. & Furthmüller, J. Efficient iterative schemes for ab initio total-energy calculations using a plane-wave basis set. Phys. Rev. B 54, 11169 (1996).
41. Perdew, J. P., Burke, K. & Ernzerhof, M. Generalized gradient approximation made simple. Phys. Rev. Lett. 77, 3865–3868 (1996).
42. Yuan, Q. H., Hu, H. & Ding, F. Threshold Barrier of Carbon Nanotube Growth. Phys. Rev. Lett. 107, 156101 (2011).
43. Yuan, Q., Xu, Z., Yakobson, B. I. & Ding, F. Efficient Defect Healing in Catalytic Carbon Nanotube Growth. Phys. Rev. Lett. 108, 245505 (2012).

Acknowledgments

Author contributions

Q.H. Yuan and G.Y. Song carried out the theoretical calculations. Q.H. Yuan prepared all the figures. F. Ding and Q.H. Yuan analyzed the data and wrote the main manuscript text. All authors discussed the results and commented on the manuscript.

Additional information

Supplementary information accompanies this paper at http://www.nature.com/scientificreports

Competing financial interests: The authors declare no competing financial interests.

How to cite this article: Yuan, Q., Song, G., Sun, D. & Ding, F. Formation of Graphene Grain Boundaries on Cu(100) Surface and a Route Towards Their Elimination in Chemical Vapor Deposition Growth. Sci. Rep. **4**, 6541; DOI:10.1038/srep06541 (2014).